SOUTH POLAR COLOR ANALYSES OF THE MOON BY KAGUYA MI. H. Sato[1], M. Ohtake[2], [1]Japan Aerospace Exploration Agency, 3-1-1 Yoshinodai, Chuo-ku, Sagamihara, Kanagawa, Japan (sato.hiroyuki@jaxa.jp), [2]ARC-Space, the University of Aizu, Japan.

Introduction: Due to the systematically increasing incidence angle toward the pole, it has been challenging to obtain reliable reflectance spectra in lunar polar regions. On the other hand, the low-sun results in many permanently shadowed regions (PSRs) where a rich amount of water ice is expected. Knowledge of the rock compositions and geological structures of the lunar polar region will provide important insights for the upcoming exploration missions to the Moon.

In this study, we derived a south polar color mosaic with more accurate spectral values than the pre-existing mosaics from the SELENE (Kaguya) Multi-band Imager (MI) datasets. Then we performed spectral analyses of the south pole.

Methodology: We used the MI images that have nine bands from 415 to 1550 nm with pixel resolution about 20 m/pixel in visible and 62 m/pixel in near-infrared ranges [1]. For all the images acquired above 60°S, about ~40,000 images in total, we converted the DN value to the radiance factor (***I/F***) and computed the incidence (***i***), emission (***e***), and phase (***g***) angles of each pixel based on the local topography using the digital terrain models (DTMs) from Kaguya Terrain Camera (TC) and Lunar Orbiter Laser Altimeter (LOLA) datasets [2]. The misalignment between the images caused by the low accuracy of the spacecraft positioning information was minimized by matching the LOLA DTM and the MI's stereo DTM [3].

For the photometric normalization, we derived the Hapke parameters from the MI images acquired at two sampling sites. One is the Apollo 16 standard site (A16StS, Fig.1) that has been widely used as an optical standard in multiple previous studies [e.g.,4-6]. Since the MI observations at A16StS are limited in ***g*** and ***i*** up to ~45° (Fig.2), we added larger-angle observations from another sampling site near 60°N (hereafter called "StS2", Fig.1) to improve the accuracy of photometric normalization of the high-latitude images. The StS2 is spectrally similar to the A16StS based on the gridded map of Kaguya Spectral Profiler (SP) data [7].

We computed the photometrically normalized ***I/F*** (***nI/F***) of all the MI observations and derived a median value for each pixel of our new polar mosaic. This achieves a higher signal-to-noise ratio and reduced normalization errors than a mosaic using single observations. We then performed the principal component analyses (PCA) of the new color mosaic and mapped the geologic units based on the horizontal variations.

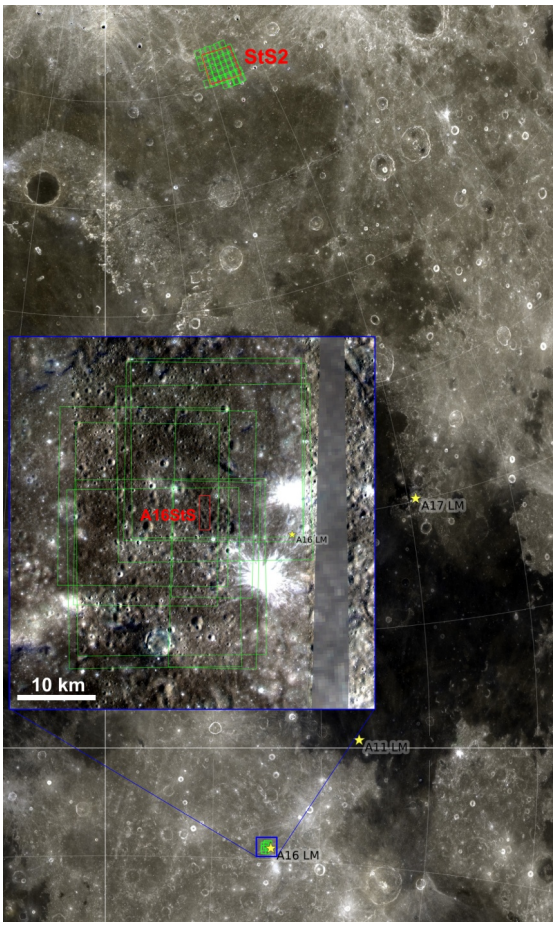

Figure 1. The locations of the sampling sites, A16StS and StS2 (red boxes), of the Hapke parameter calculations. Yellow star and green box indicate the Apollo landing sites and the footprints of the MI images that include the sampling sites, respectively. The basemap is LROC WAC color composite (R:689, G:604, B:415 nm), and the inset image is the MI color composite v3.0 (R:950, G:750, B:415 nm).

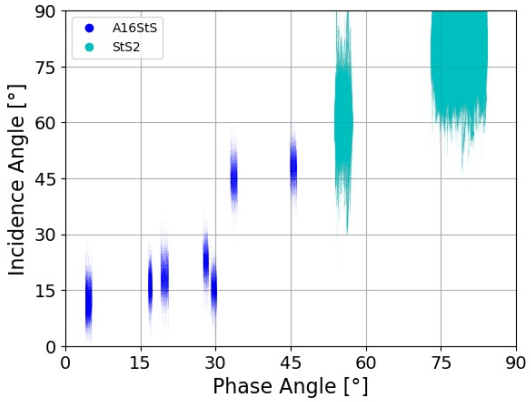

Figure 2. The phase and incidence angle variations of the MI images (415 nm band) from the two sampling sites.

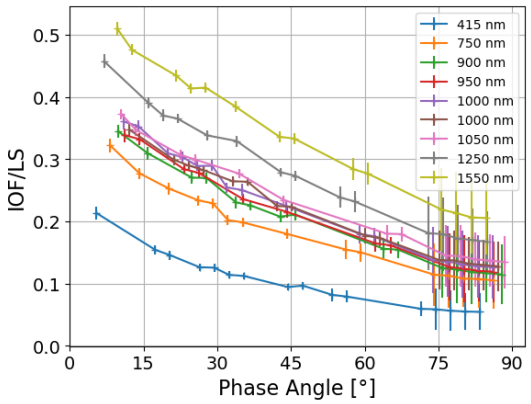

Figure 3. The phase curves of the sampling sites in nine bands from 415 to 1550 nm, observed by the MI. Errorbar indicates the standard deviation of each 3° bin. The ***IOF/LS*** denotes the ***I/F*** divided by the Lommel-Seeliger function [8], which can reduce the effects of the ***i*** and ***e*** variations.

Results: The phase curves based on the mixed observations of two sampling sites (Fig.3) show smooth decay toward the larger ***g*** angle without noticeable offset, indicating that the spectral- and probably the photometric- properties of the StS2 are similar to the ones of the A16StS. Extending the angle ranges in this method allows us to accurately normalize the high-latitude observations by the small ***i*** and ***g*** angles, such as the traditional 30°.

The mapping of the south pole region based on the PCA revealed that the ejecta and rays from relatively large craters (e.g., Schomberger A and Grotrian, Fig.4, bottom) are about 2-5 times more extensive than described in the latest USGS geologic map [9] (Fig.4, top). The rays from Tycho crater traverse over 5,000 km near the south pole and intersect the ejecta of Shackleton crater. We also found many highly reflective ejecta deposits spread around relatively young craters (Fig.4, on average 5-6 km in diameter with no name in the IAU database). Most of these ejecta are not visible in the topographic reliefs. Some are not even distinguishable from single-band reflectance or composite colors but only visible in the PCA, suggesting that those ejecta do have spectral differences relative to the background materials. Knowledge of these detailed geologic structures could provide critical constraints on the origin of samples obtained by future landing expeditions.

Discussion: The variation of photometric properties in the polar region was already reported by [10], indicating that the single parameter set is not optimum for the entire polar region. The development of a spectral library with rich angle various, particularly the larger angles, will allow us more accurate spectral analyses in the lunar polar regions.

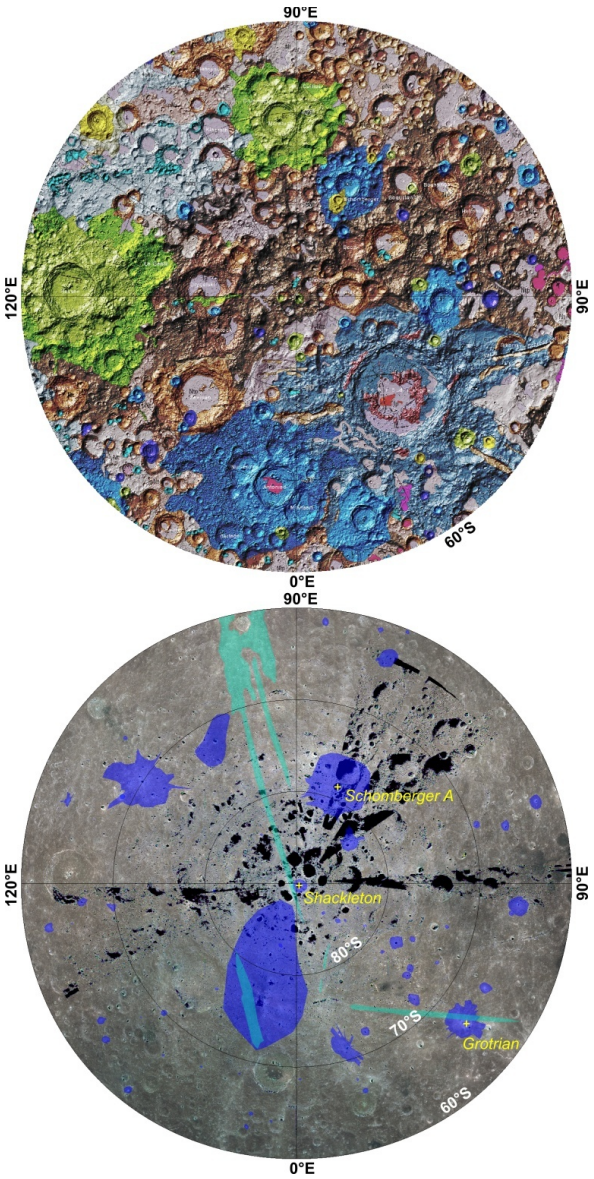

Figure 4. U.S. Geological Survey (USGS) Global Lunar Geologic Map released in 2020 [9] (top), and the distribution of relatively young ejecta (blue) and rays (cyan) mapped by the PCA of our new mosaic (bottom).

References: [1] Kodama, S. et al. (2010) *Space Sci. Rev.*, v154, 1-4, p79-102. [2] Smith et al. (2010) *GRL*, 37(18). [3] Sato et al. (2020) *Japanese Society of Planetary Sciences*, *Fall meeting* #O-D1-B16. [4] Ohtake et al. (2010) *Space Science Reviews*, v154, issue 1-4, p57-77. [5] Yamamoto et al. (2011) *IEEE Transactions on Geoscience and Remote Sensing*, v49, p4660-4676. [6] Pieters (1999) *New Views ofthe Moon II Workshop*, v8025, 1999. [7] Hareyama et al. (2019) *Icarus*, v321, p407-425. [8] Hapke (2012) *Cambridge Univ. Press*, NY. [9] Fortezzo et al. (2020) 51st LPSC, abstract #2760. [10] Sato et al. (2018) 49th LPSC, abstract #1511.